

Morphological Diversity and Nanofiber Networks of Poly(*p*-oxybenzoyl) generated by Phase Separation during Copolymerization

Toshimitsu Ichimori,¹ Kenta Mizuma,¹ Tetsuya Uchida,² Shinichi Yamazaki,¹ Kunio Kimura¹

¹Division of Sustainability of Resources, Graduate School of Environmental Science, Okayama University,
3-1-1 Tushima-Naka Kita-Ku, Okayama, 700-8530 Japan

²Division of Chemistry and Biotechnology, Graduate School of Natural Science and Technology, Okayama University,
3-1-1 Tushima-Naka Kita-Ku, Okayama, 700-8530 Japan

Correspondence to: K. Kimura (E-mail: polykim@cc.okayama-u.ac.jp)

ABSTRACT: Poly(*p*-oxybenzoyl) (POB) precipitates prepared by reaction-induced phase separation during copolymerization exhibit wide variety of morphologies such as fibril, needle, slab, spindle, and sphere. The morphology is significantly influenced by the copolymerization conditions of structure of trifunctional comonomers, copolymerization ratio, solvent, concentration, and temperature of the polymerization. Among them, POB nanofiber networks like a texture of nonwoven fabrics are obtained only by the polymerization of 4-acetoxybenzoic acid with 3,5-diacetoxybenzoic acid (DABA) in aromatic solvent at a concentration of 1.0–2.0% at the content of DABA in feed of 10–20 mol % at 320°C. The network is comprised of fibrillar crystals connected each other at spherical nodal points. The diameters of the fibers are 90–129 nm. This network is highly crystalline and the molecules are aligned along the long direction of the fibers. Various parameters characterized the networks can be controlled by the polymerization concentration.

© 2012 Wiley Periodicals, Inc. J. Appl. Polym. Sci. 000: 000–000, 2012

KEYWORDS: polyesters; fibers; morphology; phase behavior; crystallization

Received 1 August 2012; accepted 4 September 2012; published online

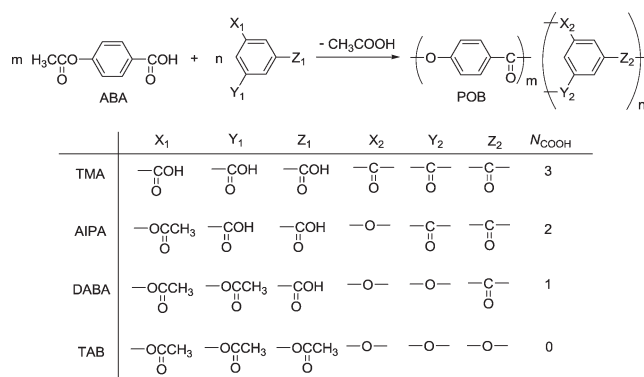
DOI: 10.1002/app.38554

INTRODUCTION

Rigid aromatic polymers exhibit the outstanding performances under unusual and demanding operating conditions, and they have been paid much attention from industrial aspects. The function and performance of the materials are highly related to the morphologies with molecular orientation, and the morphological diversity is one of powerful tools and keys to elaborate the sophisticated and functional system in nature. It was found in recent years that materials down-sized to the nanometer scale can show very different properties enabling unique applications,^{1–3} and various morphologies such as spheres, fibers, ribbons and others have been developed so far. Among them, nanofiber networks like nonwoven fabrics attract much interest because of their potential applications in many fields, such as protective clothing, high performance filters, and high strength fillers for polymer composites.^{4–9} Hence, as one kind of high-performance materials, nanofiber networks of rigid aromatic polymers will become more indispensable in a high-technology field. Some of the aromatic polymers such as polyimides,^{10–14} polyamides,^{15–17} polybenzimidazoles,¹⁸ and polybenzoxazoles^{13,19,20} can be electrospun into nanofibers by using soluble precursors. However, many of them comprised of rigid-rod structures are usually insol-

uble in common organic solvents and infusible. Owing to their intractability, they could not be directly electrospun into the nanofiber networks.

Reaction-induced phase separation during isothermal solution polymerization is an attractive another stream for making nanofibers and their networks. The morphology is created by the phase-separation of oligomers, and therefore this method is no longer limited by the intractability of rigid polymers.^{21–24} Poly(*p*-oxybenzoyl) (POB) whiskers had been prepared by the polymerization of 4-acetoxybenzoic acid (ABA) in liquid paraffin (LPF) and aromatic solvents.^{22,23} The POB whiskers were formed by the crystallization of oligomers and subsequent polymerization in the precipitated crystals. The unique microspheres having needle-like crystals on the surface have been also prepared by the polymerization of ABA with 3,5-diacetoxybenzoic acid (DABA).²⁵ In this case, the liquid–liquid phase separation was first induced in the initial stage of the polymerization to form microspheres. Next the crystallization of oligomers started on the surface of the already formed microspheres after the middle stage of the polymerization, resulting in the formation of the needle-like crystals on the surface of the microspheres. Networks of spheres had been prepared by the polymerization



Scheme 1. Copolymerization of ABA with four different trifunctional comonomers.

of ABA with DABA, in which the large spheres connected each other by the fibrillar crystals.²⁶

It needs to clarify the influence of the polymerization conditions on the morphology systematically not only for the preparation

of the POB nanofiber network but also for the control of its structure from the view point of the morphological diversity. This study aims to investigate the details of the influence of the structure of the trifunctional comonomer, its copolymerization ratio, the solvent, the concentration and the temperature of the polymerization on the morphology of the POB precipitates.

EXPERIMENTAL

Materials

ABA was purchased from TCI and purified by recrystallization from ethyl acetate. Trimesic acid (TMA) was purchased from TCI and purified by the recrystallization from methanol. 5-Acetoxyisophthalic acid (AIPA) was synthesized by the acetylation of 5-hydroxyisophthalic acid purchased from TCI with acetic anhydride according to the previous procedure.²⁷ Triacetoxymethylbenzene (TAB) was also synthesized by the acetylation of phloroglucinol purchased from TCI with acetic anhydride according to the previous procedure.²⁸ DABA was synthesized and purified according to previous procedures.^{25,26} LPF was purchased from Nacalai Tesque, and purified by vacuum

Table I. Results of Polymerization ABA with Trifunctional Comonomers

Run no.	Polymerization condition ^a			Yield (%)	χ_p^c (mol %)	Morphology
	Solvent	Comonomer	χ_f^b (mol %)			
1	LPF	TMA	1	41	<0.1	Sphere
2	LPF	AIPA	1	44	<0.1	Fibril
3	LPF	AIPA	5	36	7.6	Sphere
4	LPF	AIPA	10	14	11.0	Sphere
5	LPF	AIPA	20	16	18.0	Sphere
6	LPF	DABA	5	56	6.4	SN ^d
7	LPF	DABA	10	48	9.8	SN
8	LPF	DABA	20	43	18.2	SN
9	LPF	TAB	10	29	<0.1	Fibril
10	DBT	TMA	1	32	<0.1	Spindle
11	DBT	TMA	5	31	1.3	SN
12	DBT	TMA	10	32	8.2	Sphere
13	DBT	TMA	20	12	12.0	Sphere
14	DBT	AIPA	1	29	<0.1	Slab
15	DBT	AIPA	5	43	1.8	Slab, sphere
16	DBT	AIPA	10	52	13.1	Sphere
17	DBT	AIPA	20	45	14.6	Sphere
18	DBT	DABA	5	47	1.2	Fibril
19	DBT	DABA	10	28	1.0	Network
20	DBT	DABA	15	49	2.0	Network
21	DBT	DABA	20	66	15.0	Network
22	DBT	DABA	30	47	24.6	Sphere, needle
23	DBT	TAB	5	47	<0.1	Slab, fibril
24	DBT	TAB	10	36	<0.1	Slab, fibril
25	DBT	TAB	20	16	<0.1	Slab, fibril

^aPolymerization was carried out at a concentration of 1.0% at 320°C for 6 h.

^bMolar ratio of trifunctional comonomer in feed (χ_f) (mol %) = [trifunctional comonomer]/([trifunctional comonomer] + [ABA]) \times 100.

^cMolar ratio of trifunctional comonomer moiety in product (χ_p) (mol %) = [trifunctional comonomer moiety]/([trifunctional comonomer moiety] + [4-oxybenzoyl moiety]) \times 100.

^dSN stands for a sphere having needlelike crystals on a surface.

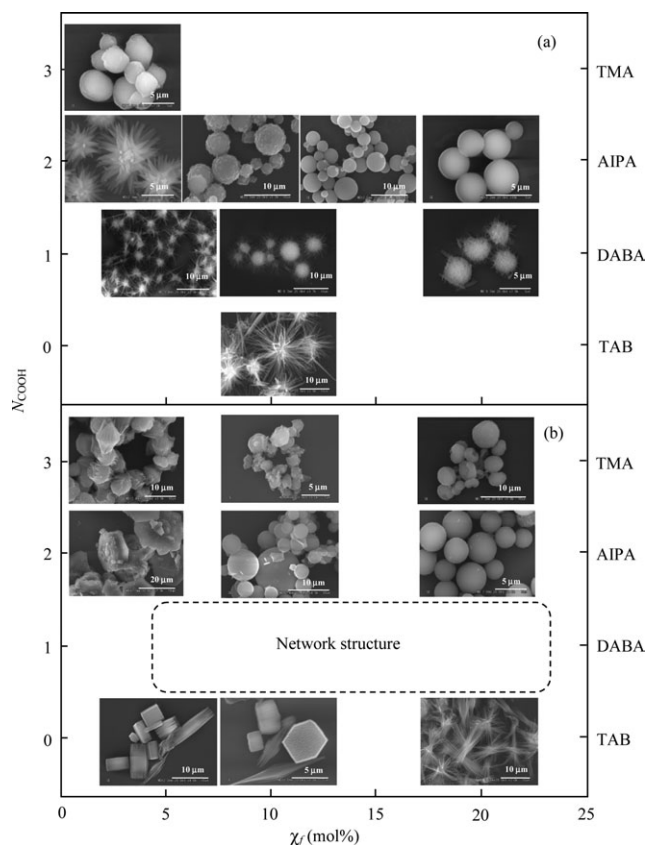


Figure 1. Morphology of precipitates prepared from ABA and various comonomers at 320°C for 6 h at a concentration of 1.0% in (a) LPF and (b) DBT presented in Table I.

distillation (220–240°C/0.3 mmHg). A mixture of isomers of dibenzyltoluene (DBT) was purchased from Matsumura Oil (Trade name: Barrel Therm 400, MW: 380, b.p.: 382°C) and purified by distillation under reduced pressure (170–180°C/0.3 mmHg).

Measurements

Morphology of the precipitate was observed on a HITACHI S-3500 N scanning electron microscope (SEM). Samples for SEM were dried, sputtered with platinum/palladium and observed at 20 kV. Average shape parameters of the products were determined by taking the average of over 100 observation values. Morphology and selected area electron diffraction (SAED) were performed on a JEM 2000EX transmission electron microscope (TEM). Samples for TEM were prepared by depositing the precipitate suspension in acetone onto carbon grids and drying in air at 25°C and observed at 200 kV. Infrared (IR) spectra were recorded on a JASCO FT/IR-410 spectrometer. Wide angle X-ray scattering (WAXS) was performed on a Rigaku Gaiger Flex with nickel-filtered CuK α radiation (35 kV, 20 mA). The content of trifunctional comonomer moiety in the precipitates (χ_p), defined as [trifunctional comonomer moiety]/([trifunctional comonomer moiety] + [4-oxybenzoyl moiety]) \times 100 mol %, was determined by high performance liquid chromatography (HPLC) analysis after hydrolysis according to the previously reported procedure.^{25,26}

Polymerizations

ABA (0.25 g, 1.39 mmol), DABA (0.058 g, 0.245 mmol), and 20 mL of DBT were placed into a cylindrical vessel equipped with a mechanical stirrer and a gas inlet and outlet tubes. The reaction mixture was heated up to 320°C with stirring under a slow stream of nitrogen. The stirring was stopped when the monomers were completely dissolved. The reaction mixture was kept at 320°C for 6 h. The solution became turbid, and then the polymer products were formed as precipitates. The polymer precipitates were collected by vacuum filtration at 320°C, and washed with *n*-hexane and acetone. IR of the precipitates (KBr, cm⁻¹): 3075, 1736, 1599, 1507, 1445, 1415, 1256, 1199, 1154, 1046, 1011, 885, 757.

Polymerizations of ABA with other trifunctional comonomers and those under different conditions without stirring were carried out in the similar manner.

A polymerization under stirring was carried out as follows; ABA (0.38 g, 2.08 mmol), DABA (0.088 g, 0.367 mmol), and 20 mL of DBT were placed into a cylindrical vessel equipped with a mechanical stirrer and a gas inlet tube. The stir bar was a rod type, of which the diameter was 2.8 cm and the clearance between the inner wall of the cylindrical vessel and stir bar was 3 mm. The reaction mixture was heated under a slow stream of nitrogen up to 320 °C with stirring speed of 300 rpm, of which the shear rate ($\dot{\gamma}$) was 147 s⁻¹. The temperature was maintained at 320 °C for 6 h. The precipitates were collected by vacuum filtration at 320 °C and washed with *n*-hexane and acetone.

RESULTS AND DISCUSSION

Influence of Trifunctional Comonomer on Morphology

Four kinds of trifunctional comonomers were polymerized with ABA as shown in Scheme 1 to clarify the influence of the structure of the trifunctional comonomer on the morphology. Here, the number of carbonyl group in the trifunctional comonomer

Table II. Results of Polymerization ABA with DABA at Various χ_f s and Temperatures

Run no	Polymerization condition ^a		Yield (%)	χ_p^c (mol %)	Morphology
	χ_f^b (mol %)	Temperature (°C)			
26	10	280	28	< 0.1	Fibril
27	15	280	58	13.8	Network
28	15	360	67	<0.1	Fibrillated slab
29	20	280	69	14.4	Network, SN ^d
30	20	360	60	<0.1	Slab, needle
31	30	280	22	15.3	Fibrillated bundle

^aPolymerizations were carried out in DBT at a concentration of 1.0% for 6 h.

^bMolar ratio of DABA in feed (χ_f) (mol %) = [DABA]/([DABA] + [ABA]) \times 100.

^cMolar ratio of 3,5-dioxybenzoyl moiety in product (χ_p) (mol %) = [3,5-dioxybenzoyl moiety]/([3,5-dioxybenzoyl moiety] + [4-oxybenzoyl moiety]) \times 100.

^dSN stands for a sphere having needlelike crystals on a surface.

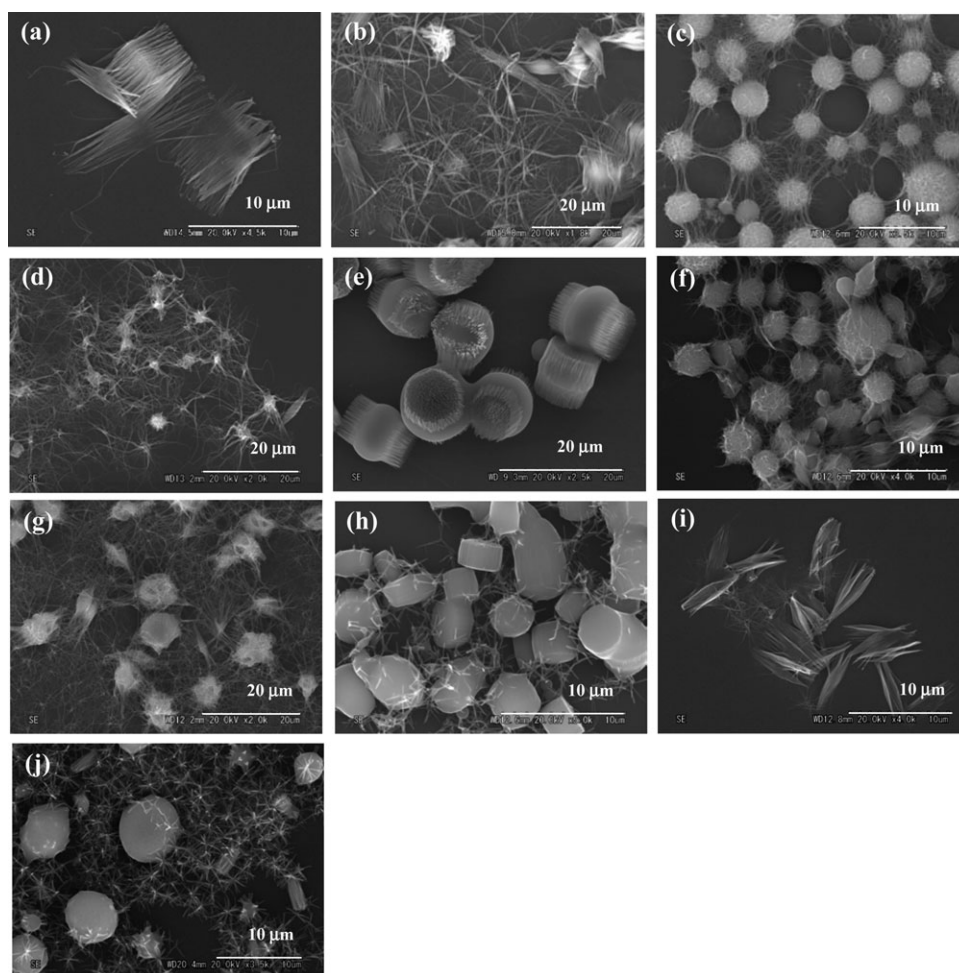


Figure 2. Morphology of precipitates prepared from ABA and DABA in DBT at various χ_f values and temperatures. (a) χ_f of 10 mol % and 280°C (run no. 26), (b) χ_f of 10 mol % and 320°C (run no. 19), (c) χ_f of 15 mol % and 280°C (run no. 27), (d) χ_f of 15 mol % and 320°C (run no. 20), (e) χ_f of 15 mol % and 360°C (run no. 28), (f) χ_f of 20 mol % and 280°C (run no. 29), (g) χ_f of 20 mol % and 320°C (run no. 21), (h) χ_f of 20 mol % and 360°C (run no. 30), (i) χ_f of 30 mol % and 280°C (run no. 31), and (j) χ_f of 30 mol % and 320°C (run no. 22).

(N_{COOH}) changed from 0 to 3, that is, TAB ($N_{\text{COOH}} = 0$), DABA ($N_{\text{COOH}} = 1$), AIPA ($N_{\text{COOH}} = 2$) and TMA ($N_{\text{COOH}} = 3$).

Polymerizations were carried out in LPF and DBT at a concentration of 1.0% at 320°C for 6 h without stirring. Results of polymerization are presented in Table I and morphologies of the precipitates are shown in Figure 1. ABA and these trifunctional comonomers were not dissolved in the solvents at 25°C, but they

became dissolved during heating to 320°C. The solubility of the trifunctional comonomer depends on the structure, and it decreased with the N_{COOH} value. In LPF, the polymerizations of TMA and AIPA mainly afforded the spheres. Those of DABA gave the sphere having needlelike crystals on a surface at χ_f of 5–20 mol % as previously reported.²⁵ The polymerization of TAB afforded the fibrillar crystals even at χ_f of 10 mol %. In this polymerization, the yield of

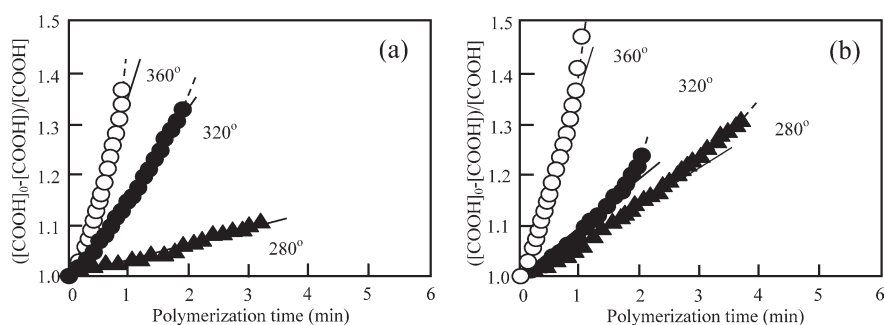


Figure 3. Kinetics of reactions of (a) ABA and (b) DABA in DBT at an initial concentration of 83.3 mmol L^{-1} at various temperatures.

Table III. Kinetic Parameters of Reaction of ABA and DABA^a

Monomer	k_2 (10^{-1} L mol ⁻¹ min ⁻¹)			Activation energy (kJ mol ⁻¹)
	280°C	320°C	360°C	
ABA	0.52	2.02	4.84	83
DABA	1.46	2.47	5.71	45
k_2 DABA/ k_2 ABA	2.81	1.22	1.18	

^aPolymerizations were carried out in DBT at an initial concentration of 83.3 mmol L⁻¹.

29% was lower than that of other polymerizations and the χ_p value was less than 0.1 mol %. The solubility of oligomers is strongly influenced by the structure of the end-groups and it increases with the content of acetoxy group. The oligomers containing TAB moiety could not be precipitated because of the high solubility and the oligomers not containing 1,3,5-trioxybenzene moiety were mainly precipitated to form the fibrillar crystals. Owing to this, the network structure was not formed in LPF.

The polymerizations in DBT yielded the precipitates having various morphologies such as spindle-like crystals, slab-like crystals, fibrillar crystals, and spheres depending on the polymerization conditions, but the network was formed only in the polymerization of ABA with DABA at χ_f of 10–20 mol %. The crystals having clear habits like slab and fibril were formed mainly in the polymerization with TAB in DBT as well as in LPF. In both solvents, the morphology changed from the spheres to the crystals having clear habit with the decrease in the N_{COOH} value. This morphological change can be understood as follows; when the N_{COOH} value is higher than one, the co-oligomers containing 5-carboxyisophthaloyl moiety and 5-oxyisophthaloyl moiety corresponding to TMA and AIPA residue are phase-separated via liquid–liquid phase separation resulting in the formation of microspheres, because the solubility of oligomers increases with the decrease in the N_{COOH} value derived from the structure of the end-group. In contrast to this, when the N_{COOH} value is zero, the co-oligomers containing 1,3,5-trioxybenzene moiety corresponding to TAB residue cannot be precipitated because of the higher solubility. Therefore, the oligomers comprised of 4-oxybenzoyl moiety are crystallized to form the crystals having clear habits like slabs, spindles and needles. When the N_{COOH} value is two, the phase separation mode is changed from the liquid–liquid phase separation to the crystallization during polymerization. One possibility for the formation mechanism of the network had been already proposed.²⁶ Oligomers containing 3,5-dioxybenzoyl moiety corresponding to DABA residue are precipitated via liquid–liquid phase separation to form the microdroplets in the initial stage of the polymerization. The microspheres are formed by the solidification of the droplets caused by the further polymerization in them. During this solidification process, the fibrillar crystals are developed by the crystallization in the coalesced spheres. Some of the co-oligomers containing 3,5-dioxybenzoyl moiety are eliminated from the spheres by both the segregation effect and the ester–ester exchange reaction. The fibrillar crystals connecting the spheres appear consequently owing to the shrinkage of the spheres. The oligomers comprised of 4-oxybenzoyl moiety are then phase-separated by crystallization after the

middle stage of the polymerization, and the fibrillar crystals grow on the surface of the spheres. The shrunk spheres are left as nodal points in the networks. Based on this mechanism, both the formation of droplet via liquid–liquid phase separation and the consequent development of the fibers by crystallization in the coalesced spheres are of importance to form the network. It becomes clear that DABA ($N_{\text{COOH}} = 1$) is the desirable trifunctional comonomer to prepare networks and DABA acts as a liquid–liquid phase separation inducer.

Influence of Temperature and χ_f Value on Morphology

Next, the polymerizations of ABA with DABA in DBT were carried out at a concentration of 1.0% for 6 h at 280 and 360°C with varying the χ_f value from 10 to 30 mol %. Results of the polymerization are presented in Table II and the morphologies of the precipitates are shown in Figure 2.

The morphology was significantly influenced by the temperature and the χ_f value. When the polymerization temperature was 280°C, the network was formed at χ_f of 15 and 20 mol %. In contrast to this, the precipitates prepared at 360°C exhibited clear crystal habits. The χ_p values of them were less than 0.1 mol %, indicating that the crystals prepared at 360°C were comprised of only 4-oxybenzoyl moiety. On the basis of these results, it concludes that the desirable χ_f values for the preparation of the network at 280°C and 320°C were 15–20 mol % and 10–20 mol %, respectively. The phase separation mode in the copolymerization

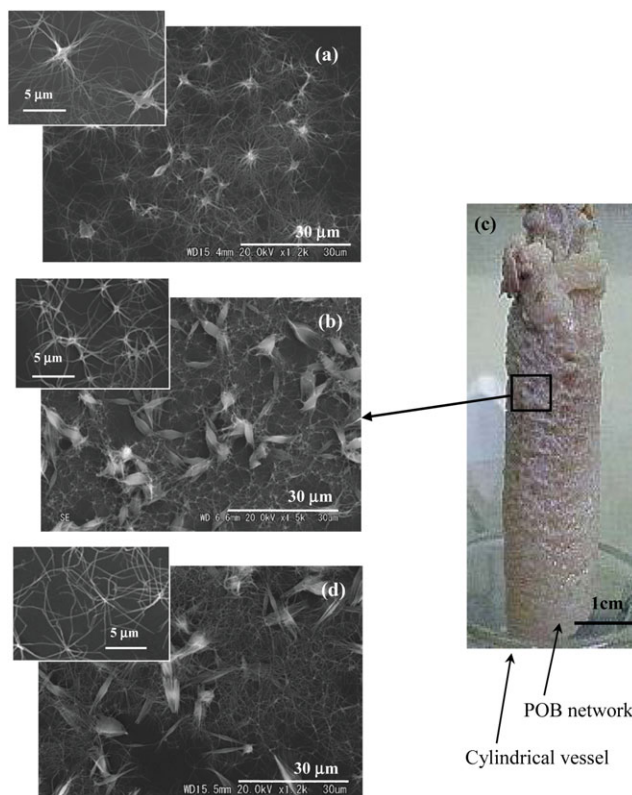


Figure 4. Feature of as-prepared POB network and SEM micrographs of POB network prepared from ABA and DABA at a concentration of (a) 1.0%, (b, c) 1.5%, and (d) 2.0%. Polymerizations were carried out in DBT at χ_f of 15 mol %, and 320°C for 6 h.

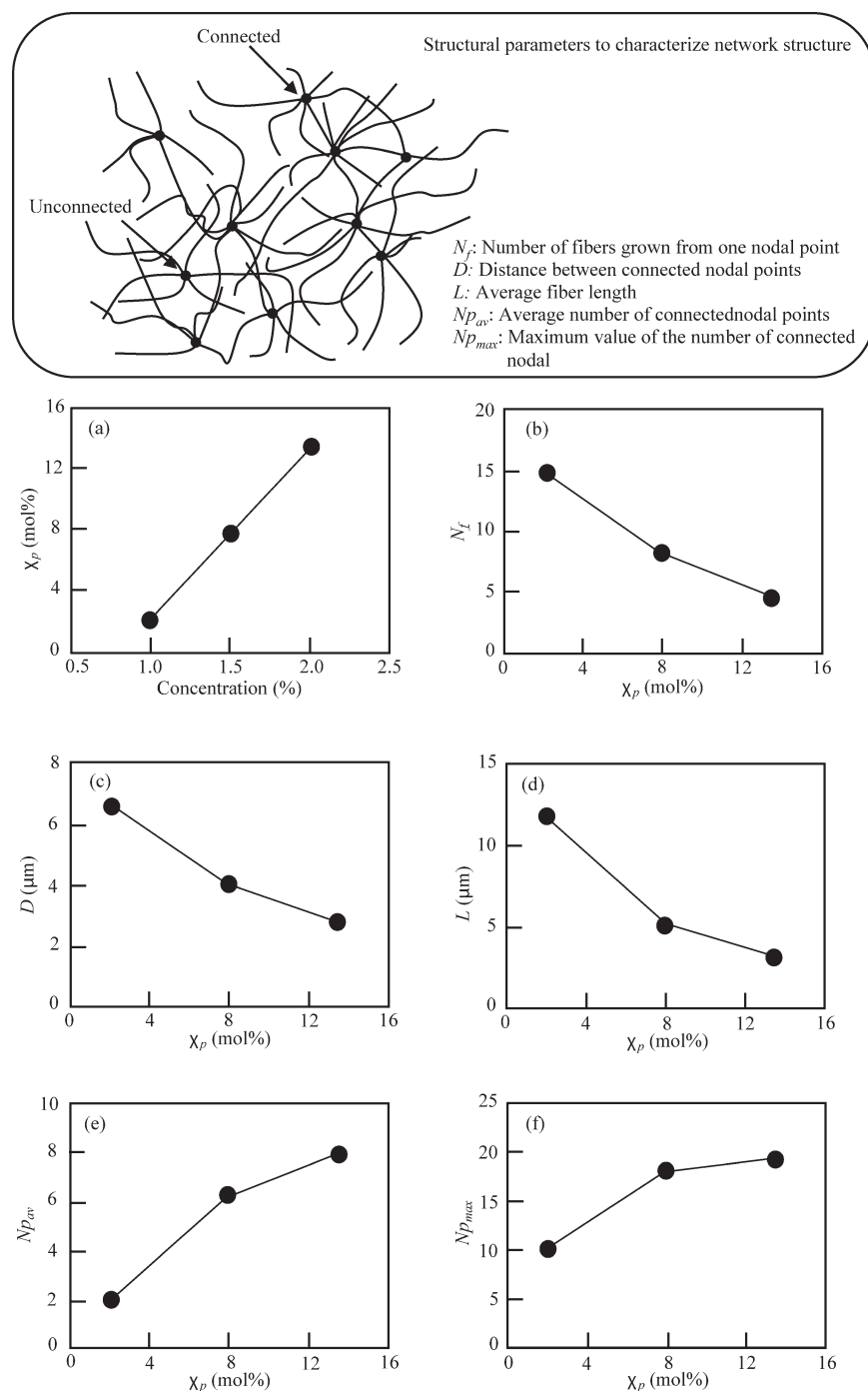


Figure 5. Plots of various parameters of POB networks prepared from ABA and DABA in DBT for 6 h at χ_f of 15 mol %, 320°C, and concentrations of 1.0, 1.5, and 2.0%; (a) concentration vs. χ_p , (b) χ_p vs. N_f , (c) χ_p vs. D , (d) χ_p vs. L , (e) χ_p vs. $N_{p_{av}}$, and (f) χ_p vs. $N_{p_{max}}$.

system is determined by the solubility of oligomers dependent on their composition. Reaction rates of ABA and DABA were measured at 280, 320, and 360°C until the oligomer precipitation occurred to estimate the oligomer composition formed in the initial stage of the polymerization. The results are plotted in Figure 3. The reaction at the very beginning of the polymerization before the phase separation obeyed second-order kinetics. The rate constants of the second-order reaction (k_2) and the activation energies are summarized in Table III.

The k_2 values of the both reactions naturally increased with the temperature. Although the k_2 of the reaction DABA was larger than that of ABA, the activation energy of the reaction ABA was 1.84 times larger than that of DABA. Owing to this, the ratio of k_2 of DABA and ABA decreased with the increase in the temperature. This tendency suggests that the oligomers containing more 3,5-dioxybenzoyl moiety are formed at higher temperature in the initial stage of polymerization. To induce the liquid-liquid phase separation, the formation of the oligomers containing

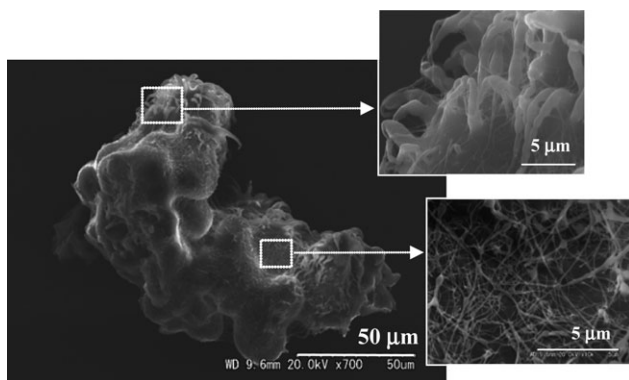


Figure 6. Morphology of precipitated polymers prepared from ABA and DABA in DBT at χ_f of 15 mol %, and 320°C for 6 h under shearing. Concentration was 1.5% and γ was 147 s⁻¹.

3,5-dioxybenzoyl moiety is needed because the 3,5-dioxybenzoyl moiety shifts the freezing point of the oligomers toward lower temperature, and the higher temperature is likely desirable from the view point of the reaction rate. However, the χ_p value of the precipitates prepared at 360°C was less than 0.1 mol % and the precipitates exhibited very clear crystal habits, indicating clearly that the oligomers containing 3,5-dioxybenzoyl moiety could not be phase-separated because of their higher solubility. The temperature of 360°C was too high to induce the liquid-liquid phase separation. The structural homogeneity of the network prepared at χ_f of 15 mol % at 320°C is the highest among the networks prepared under various conditions.

Control of Network Structure

Monomer concentration is also an important factor to influence the morphology. The polymerizations of ABA with DABA were carried out at χ_f of 15 mol % in DBT at 320°C for 6 h with varying the concentration from 1.0 to 2.0% to clarify the influence of the concentration on the network structure. The morphologies of prepared networks are shown in Figure 4.

As-polymerized networks contained DBT. The network was composed of the fibrillar crystals connected together at nodal points.

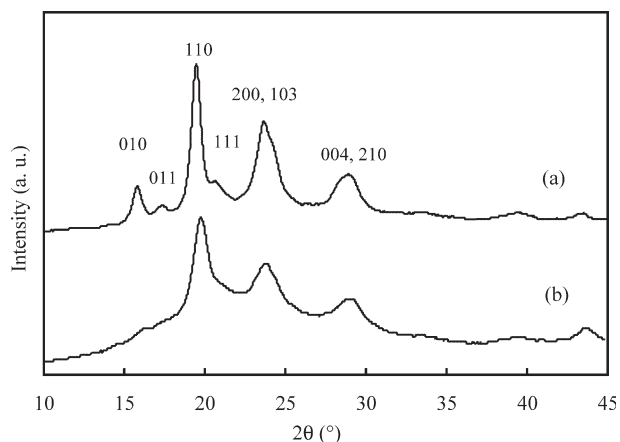


Figure 7. WAXS intensity profiles of products prepared from ABA and DABA in DBT for 6 h at χ_f of 15 mol %, a concentration of 1.5%, and at (a) 320°C and (b) 280°C.

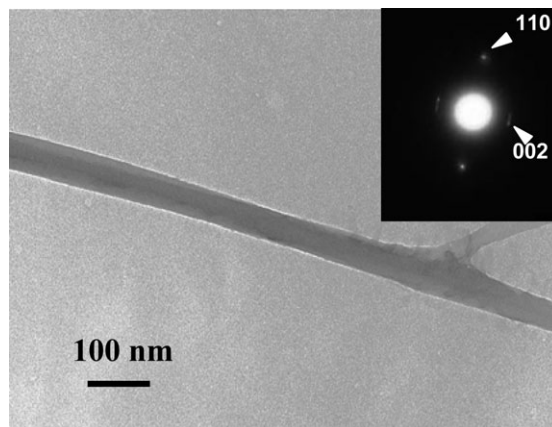


Figure 8. TEM image and SAED pattern of a fiber in POB networks prepared from ABA and DABA in DBT at χ_f of 15 mol %, 320°C, and a concentration of 1.5% for 6 h.

The average diameters of the fibrillar crystals prepared at concentrations of 1.0, 1.5, and 2.0% were 129, 90, and 108 nm, respectively. The diameter was not influenced by the concentration. The obtained nanofiber networks resemble the texture of nonwoven fabrics prepared by the conventional methods. Although the fibrillated bundle crystals were hardly formed at a concentration of 1.0%, they were done in the networks prepared at concentrations of 1.5 and 2.0%. The average length and width of the bundle crystals prepared at a concentration of 1.5% were 7 and 2 μm , respectively. Those at a concentration of 2.0% were 12 and 4.5 μm , respectively. The size of the bundle crystals increased with the concentration. In order to characterize the networks, various parameters of the network structure are plotted as a function of the χ_p value in Figure 5. The χ_p value of the network depended on the concentration and it increased with the concentration as shown in Figure 5(a). The number of fibers grown from one nodal point (N_p), the distance between connected nodal points (D) and average fiber length (L) decreased with the χ_p value, and the average number of connected nodal points (N_{pav}) and the maximum value of the number of connected nodal points (N_{pmax}) increased with the χ_p value. The nodal points were connected by several nanofibers at intervals of 3–7 μm in the network. It is reasonably understood that higher concentration made the size smaller and the number of the droplet larger because the nucleation occurred via the higher super-saturated state of oligomers.^{29,30} According to the formation mechanism, the structure of connected droplets is an embryonic structure for the networks, and therefore smaller size of the droplets results in the smaller D and the larger number of connected nodal points (N_p).

In order to increase the N_{pav} value and to decrease the diameter of the fiber, the stirring was applied to the polymerization of ABA with DABA at χ_f of 15 mol % at a concentration of 1.5% in DBT at 320°C. It has been reported that the stirring accelerated the fibrillation of the POB whiskers to yield the fibrillated fine fibers.³¹ The precipitates were obtained under stirring at γ was 147 s⁻¹ with the yield of 12%. The yield decreased by stirring. Fine fibers were locally observed on the surface of the fused spheres as shown in Figure 6, whereas the network did not developed in the polymerization under stirring.

It has been reported previously that the stirring influenced the phase-separation behavior of the oligomers and the apparent reaction rate of monomers, bringing about the change in the morphology and the composition of copolymers.³¹ The χ_p value under stirring was 7.3 mol % and it was almost the same as that without stirring of 7.9 mol %. The stirring disturbs to form and grow the microdroplets uniformly, leading to the formation of fused spheres and the inhabitation of the fibril formation.

Characterization of Networks

WAXS profiles of the networks prepared at χ_f of 15 mol % and a concentration of 1.5% are shown in Figure 7.

Sharp reflection peaks were visualized in the profile of the networks prepared at 320°C, suggesting high crystallinity. All these peaks could be indexed by the orthorhombic unit cell of the POB crystal.³² In contrast to this, the profile of the network prepared at 280°C contained diffuse halo attributed to the amorphous region besides the peaks of the POB crystals. Additionally the reflection peaks were not so sharp compared with those prepared at 320°C, suggesting that this networks prepared at lower temperature possessed lower crystallinity. The crystals developed more rapidly at higher temperature owing to the better mobility of the polymer molecules. Further, the higher polymerization temperature made the χ_p value lower as aforesaid. These effects enhanced the crystallinity at 320°C. Molecular orientation in the fibers is of importance to gain the good mechanical properties and it was analyzed by SAED. The result is shown in Figure 8. The ED pattern was not a fiber pattern of the cylindrical symmetry, and sharp spots were clearly appeared. These reflections were assigned as the POB orthorhombic crystal structure and the reflections of 002 corresponding to the c axis were observed along the long axis of the fibers. This result reveals that the POB molecules are aligned along the long direction of the fibers and this molecular orientation is desirable from the view point of fabric properties.

Thermal stability of the network prepared at χ_f of 15 mol % and a concentration of 1.5% at 320°C for 6 h was evaluated by a TGA measured in nitrogen atmosphere. The temperatures of 5 and 10% weight loss were 455 and 528°C, respectively and The POB nanofiber networks possessed excellent thermal stability.

CONCLUSIONS

Four different trifunctional comonomers were copolymerized with ABA. The morphology of the POB precipitates was significantly influenced by the structure of the trifunctional comonomer and the solvent. The POB precipitates having various morphologies such as fibrils, needles, slabs, spindles, and spheres were formed by tuning the polymerization conditions. Among them, the three dimensional nanofiber networks were obtained only by the polymerization with DABA at a concentration of 1.0–2.0% at 280–320°C in DBT. The χ_f value was of importance to prepare the networks, and that of 15–20 mol % was desirable for the polymerization at 280°C and that of 10–20 mol % for 320°C. The network structure was comprised of fibrillar crystals connected each other at spherical nodal points. The diameters of the fibrillar crystals were 90–129 nm. This network possessed

high crystallinity and the molecules were aligned along the long direction of the fibrils. The number of fibers grown from one nodal point, the distance between connected nodal points, the average fiber length and the average number of connected nodal points which characterized the network structure could be controlled by the polymerization concentration.

ACKNOWLEDGMENTS

This work was supported by a Grant-in-Aid for Scientific Research (B) (No. 21350127) from the Ministry of Education, Culture, Sports, Science and Technology, Japan.

REFERENCES

- Kanatzidis, M. G.; Wu, C. G.; Marcy, H. O.; Kannewurf, C. R. *J. Am. Chem. Soc.*, **1989**, *111*, 4139.
- Wu, C. G.; Kanatzidis, M. G.; Marcy, H. O.; DeGroot, D. C.; Kannewurf, C. R. *Polym. Mater. Sci. Eng.* **1989**, *61*, 969.
- Kanatzidis, M. G.; Wu, C. G.; Marcy, H. O.; DeGroot, D. C.; Schindler, J. L.; Kannewurf, C. R.; Benz, M.; LeGoff, E. *ACS Symp. Series* **1992**, *499*, 194.
- Dzenis, Y. *Science* **2004**, *304*, 1917.
- Gibson, P.; Schreuder-Gibson, H.; Rivin, D. *Colloids Surf. A* **2001**, *187–188*, 469.
- Bergshoef, M. M.; Vancso, G. *J. Adv. Mater.* **1999**, *11*, 1362.
- Graham, K.; Ouyang, M.; Raether, T.; Grafe, T.; McDonald, B.; Knauf, P. *Adv. Filtration Separation Technol.* **2002**, *15*, 500.
- Fong, H.; Reneker, D. H. In *Electrospinning and Formation of Nanofibers Structure Formation in Polymeric Fibers*; Salem, D. R.; Sussman, M. V., Eds.; Hanser, Munich, **2001**, p 225.
- Chen, S.; Han, D.; Hou, H. *Polym. Adv. Technol.* **2011**, *22*, 295.
- Huang, C. B.; Chen, S. L.; Reneker, D. H.; Lai, C. L.; Hou, H. Q. *Adv. Mater.* **2006**, *18*, 668.
- Chen, S. L.; Hu, P.; Greiner, A.; Cheng, C. Y.; Cheng, H. F.; Chen, F. F.; Hou, H. Q. *Nanotechnology* **2008**, *19*, 015604.
- Cheng, C. Y.; Chen, J.; Chen, F.; Hu, P.; Wu, X. H.; Reneker, D. H.; Hou, H. Q. *J. Appl. Polym. Sci.* **2010**, *116*, 1581.
- Zou, Y.; Cheng, C. Y.; Chen, J.; Greiner, A.; Hou, Q. H. *PMSE Prepr.* **2009**, *100*, 490.
- Huang, C.; Wang, S.; Zhang, H.; Li, T.; Chen, S.; Lai, C.; Hou, H. *Eur. Polym. J.* **2006**, *42*, 1099.
- Srinivasan, G.; Reneker, D. H. *Polym. Int.* **1995**, *36*, 195.
- Chen, S. L.; Hou, H. Q.; Hu, P.; Wendorff, J. H.; Greiner, A.; Agarwal, S. *Macromol. Mater. Eng.* **2009**, *294*, 265.
- Chen, S. L.; Hou, H. Q.; Hu, P.; Wendorff, J. H.; Greiner, A.; Agarwal, S. *Macromol. Mater. Eng.* **2009**, *294*, 781.
- Kim, J.-S.; Reneker, D. H. *Polym. Eng. Sci.* **1999**, *39*, 849.
- Hsu, S. L.; Lin, K. S.; Wang, C. J. *Polym. Sci. Part A: Polym. Chem.* **2008**, *46*, 8159.
- Hsu, S. L.-C.; Chang, K. C. *Polymer* **2002**, *43*, 4097.
- Kimura, K.; Kohama, S.; Yamazaki, S. *Polym. J.* **2006**, *38*, 1005.

22. Yamashita, Y.; Kimura, K. *Polymeric Materials Encyclopedia*; CRC: Boca Raton, FL, **1996**, p 8707.
23. Kricheldorf, H. R.; Schwarz, G.; Adebahr, T.; Wilson, D. *J. Macromolecules* **1993**, *26*, 6622.
24. Yan, Y.; Chen, L.; Dai, H.; Chen, Z.; Li, X.; Liu, X. *Polymer* **2012**, *53*, 1611.
25. Kimura, K.; Kohama, S.; Kondoh, S.; Yamashita, Y.; Uchida, T.; Oohazama, T.; Sakaguchi, Y. *Macromolecules* **2004**, *37*, 1463.
26. Kimura, K.; Kohama, S.; Kondoh, S.; Uchida, T.; Yamashita, Y.; Oohazama, T.; Sakaguchi, Y. *J. Polym. Sci. Part A: Polym. Chem.* **2005**, *43*, 1624.
27. Turner, S. R.; Walter, F.; Voit, B. I.; Mourey, T. H. *Macromolecules* **1994**, *27*, 1611.
28. Frich, D.; Goranov, K.; Schneggenburger, L.; Economy, J. *Macromolecules* **1996**, *29*, 7734.
29. Burton, W. K.; Cabrera, N.; Frank, F. C. *Phil. Trans. Roy. Soc.* **1951**, *A 243*, 299.
30. Frank, F. C. *Adv. Phys.* **1952**, *1*, 91.
31. Kimura, K.; Ichimori, T.; Wakabayashi, K.; Kohama, S.; Yamazaki, S. *Macromolecules* **2008**, *41*, 4193.
32. Liu, J.; Yuan, B.-L.; Geil, P. H.; Dorset, D. L. *Polymer* **1997**, *38*, 6031.